RESEARCH PAPER

PCCP
www.rsc.org/pccp

Computer simulation studies on the solvation of aliphatic hydrocarbons in 6.9 M aqueous urea solution

Daniel Trzesniak,[a] Nico F. A. van der Vegt[ab] and Wilfred F. van Gunsteren[a]

[a] *Laboratory of Physical Chemistry, Swiss Federal Institute of Technology, ETH Hönggerberg, CH-8093 Zürich, Switzerland. E-mail: daniel@igc.phys.chem.ethz.ch and wfvgn@igc.phys.chem.ethz.ch*

[b] *Max-Planck-Institute for Polymer Research, Ackermannweg 10, D-55128 Mainz, Germany. E-mail: vdervegt@mpip-mainz.mpg.de*

Received 5th November 2003, Accepted 16th December 2003
First published as an Advance Article on the web 22nd January 2004

We report solvation free energies for six aliphatic hydrocarbons in 6.9 M urea–water mixture obtained by molecular dynamics simulations. Hydrocarbon transfer free energies from water to the urea solution are also presented. Our calculations predict that, except for methane, aliphatic hydrocarbons are more soluble in 6.9 M urea than in water, in satisfactory agreement (deviations smaller than 2 kJ mol^{-1}) with experimental transfer free energies reported in the literature. An analysis of solute–solvent contributions to the solvation enthalpies and entropies indicates that urea enhances the solvation of hydrocarbons compared to pure water due to a favourable van der Waals interaction with the solute whereas the solute–solvent entropy opposes the hydrocarbon transfer. Radial distribution functions between the solute and the solvent are examined and together with an analysis based on Kirkwood–Buff theory indicate a weak preferential urea–hydrocarbon binding. The entropic penalty related with solute urea association is discussed in terms of the molecular interactions in solution.

1. Introduction

Urea is a well known protein denaturant and much used as such in protein (un)folding studies. Yet, the precise mechanism by which urea denaturates a protein is not wholly comprehended and a number of questions remain unanswered. For example, it has been debated whether urea weakens hydrophobic interactions or directly interacts with the protein amino acids by competing with intra-molecular protein hydrogen bonding.[1] Some authors support the second view,[2–4] whereas others argue that both mechanisms are equally relevant.[5,6] In a number of studies mixtures of urea and water have been analysed, both in structural terms[7–18] as well as regarding thermodynamic quantities.[19,20] Molecular dynamics (MD) simulations of proteins[21,22] or helical secondary structure elements of proteins[23] solvated in such mixtures have been carried out and analysed with an eye to the effects of urea on protein conformational stability and unfolding pathways. However in order to understand the driving forces for urea induced unfolding, it would be of interest to know the influence of urea on the solvation behaviour of individual amino acid fragments or more general on the non-polar moieties that are part of a protein. The free energy of association of methane with methane[2,24] and of urea with aromatic hydrocarbons[25] in urea–water mixtures have been investigated by Monte Carlo and MD simulations with the aim of understanding the basic interactions responsible for protein folding and denaturation. The effects that urea may have on the equilibrium aqueous solvation thermodynamics of non-polar molecules is the subject of the present study.

Strong temperature dependencies of enthalpy and entropy changes associated with non-polar solute transfer from an organic phase to water (*i.e.* large heat capacity changes of solute transfer) are characteristic for hydrophobic hydration. A second characteristic is that the transfer process is determined by an unfavourable entropy change at low temperature while being determined by an unfavourable enthalpy change at high temperature.[26] Unlike at high temperature where hydrogen bonds between water molecules are sacrificed at the expense of an unfavourable enthalpy change, at low temperatures, the tendency of water to maintain its hydrogen bonded structure prevails, a phenomenon that is expressed by the Frank and Evans model[27] that assumes water to create a low-entropy hydrogen-bonded "fence" surrounding non-polar solutes. This view has led many researchers to examine the effects of urea (and other co-solvents) on the water structure in order to elicit the microscopic origins of the effect of urea on solubilities of non-polar molecules.

Alternative views based on statistical mechanical treatments of solvation have appeared in the literature[28–33] and claim that any structural solvent reorganisation around the solute is irrelevant to solvation, and thus to hydrophobic hydration. The argument used in these studies is based on the fact that any solvent reorganisation around the solute is exactly energy-entropy compensating, therefore not contributing to the solvation free energy.[34,35] Recently, Graziano examined thermodynamic data of non-polar solute transfer from water to 7 M aqueous urea.[31,32] He concluded that hydrocarbons larger than ethane are more soluble in the urea solution than in water due to a more favourable solute van der Waals interaction energy than the opposing difference in the work of cavity formation. The work of cavity formation is the only relevant entropic contribution to the solvation free energy and was analysed based on scaled particle theory (SPT). Experimental transfer enthalpies and entropies,[36] which contain compensating solvent reorganisation contributions, are however both positive. This fact may lead one to falsely conclude that the process is driven by a favourable entropy change while being opposed by unfavourable changes of the enthalpy.

The analytical work of reference[31] has served as a motivation of our computer simulation investigations. Because

DOI: 10.1039/b314105e

we use computer simulation techniques based on atomistic force fields, our purpose has been two-fold. First, we seek to validate a recently parameterised urea–water force field[20] by reproducing experimental data of solvation in aqueous urea. Secondly, we intend to contribute to the atomic level picture of solvating non-polar solutes in this system. We report solvation free energies of methane, ethane, propane, *n*-butane, *iso*-butane, and neo-pentane in 6.9 M urea obtained by test particle insertion (methane) and thermodynamic coupling parameter integration techniques to compute free energies. The calculated solvation free energies agree satisfactorily with experimental data and reveal a strong dependence on the aliphatic hydrocarbon size in accordance with experimental and theoretical results.[24,31–33,36] In addition to the solvation free energies, we have analysed the solute–solvent contributions to the solvation enthalpies and entropies, which can be interpreted analogously to the solute–solvent interaction energy and cavity formation work reported by Graziano.[31,32] These contributions will be shown to confirm the solute–solvent energy driven salting-in (enhancement of solvation) together with the entropy driven opposition to cavity formation, theoretically predicted using scaled particle theory (SPT).[31] The relative behaviour of these quantities when varying the solute size is analysed and determines the results of the transfer process. A Kirkwood–Buff analysis[37,38] of solute–solvent radial distribution functions is presented to investigate preferential interactions between urea and the non-polar solute. To examine solvation of the solute excluded volume, cavity-solvent radial distribution functions have been calculated from MD simulations performed in the absence of attractive van der Waals forces between the solute and solvent. Differences and similarities between structural aspects of cavity solvation and the solvation of the respective solutes have recently shown to provide useful information on the extent to which the solute–solvent entropy may influence co-solvent-solute binding.[39,40]

In section 2, the theoretical methods and computational details will be described. Our simulation results are presented in section 3 and summarized in section 4.

2. Methods

All the simulations were performed using the GROMOS96 software package.[41] The 6.9 M urea–water mixture is comprised of 153 urea and 847 water molecules in a cubic box with periodic boundary conditions. The force-field parameters for this solvent mixture were taken from a urea model[20] that is compatible with the simple-point-charge (SPC) model for water.[42] The solutes were modelled based on the GROMOS96 aliphatic hydrocarbons parameterisation[43] with the exception of methane whose parameters have been described elsewhere.[39] The bond lengths were kept constant using the SHAKE algorithm[44] with a relative geometrical tolerance of 10^{-4}. The simulations were carried out at constant pressure and temperature conditions using weak coupling[45] to a thermostat with a temperature of 298 K and to a manostat with a pressure of 1 atm. The weak coupling relaxation times for the thermostat and manostat were 0.1 ps and 0.5 ps,[45] respectively. A triple-range cut-off scheme for evaluating non-bonded interactions was applied with radii of 0.8/1.4 nm, beyond 1.4 nm a reaction-field force was applied to account for the truncation of the explicit electrostatic forces. The relative dielectric permittivity of the reaction field was set to 54.[46] Inside the smaller radius the non-bonded interactions were evaluated every time step (chosen at 2 fs) whereas between the radii they were updated only every fifth time step. All systems were equilibrated for at least 500 ps before calculating the various properties. The conditions described above are the same for all simulations, unless stated otherwise. Radial distribution functions $g_{Sj}(r)$ for pairs of species S (solute) and j (solvent) were obtained from 2000 ps of simulation. The radial distribution functions were used to evaluate the Kirkwood–Buff (KB) integrals[37,38]

$$G_{Sj} = 4\pi \int_0^{R_C} \mathrm{d}r\, r^2 [g_{Sj}(r) - 1]. \qquad (1)$$

The upper integration limit R_C represents the radius of a correlation volume in which the solution structure differs from that in the bulk and thus g_{Sj} differs from unity. Denoting the number density of species (solvent) j by ρ_j, the quantity $\rho_j G_{Sj}$ is the excess coordination number of species j around the solute S and equals the difference in the number of solvent species j in the correlation volume after and before placing the solute S in the centre. In the absence of preferential solvation, the solute will expel solvent molecules from the correlation volume and $\rho_j G_{Sj}$ is negative for all solvent species j. Urea (u) binds preferentially over water (w) to the solute if $\nu = \rho_u(G_{Su} - G_{Sw})$ is positive.

The solvation free energy, solute–solvent energy/entropy, as well as the solute–solvent radial distribution functions for methane were calculated using test particle insertion (TPI).[39] A total of 125 000 methane insertions were attempted at randomly chosen positions in each of the 1000 configurations extracted from the 1000 ps system trajectory at 1 ps intervals. For the larger hydrocarbons we have used the thermodynamic integration (TI) procedure.[47,48] The TI formula for the solvation Gibbs energy, ΔG_S, is given by

$$\Delta G_S = \int_0^1 \mathrm{d}\lambda \left\langle \frac{\partial U_{uv}(\lambda)}{\partial \lambda} \right\rangle_\lambda . \qquad (2)$$

where λ is the coupling parameter, $U_{uv}(\lambda)$ denotes the potential energy function describing the total solute–solvent interaction and $\langle \cdots \rangle_\lambda$ denotes an average over an isothermal-isobaric ensemble with Hamiltonian $H(\lambda)$. It is assumed that only the solute–solvent interaction U_{uv} in the Hamiltonian H depends on λ. The parameter λ regulates the strength of U_{uv} such that $\lambda = 1$ denotes the full interaction whereas $\lambda = 0$ means none. Soft-core solute–solvent interactions were used to avoid singularities of the free energy and entropy derivatives when annihilating ($\lambda \to 0$) interaction sites.[49] The "softness" of the interaction was set by choosing the soft-core parameter[41] $\alpha_{LJ} = 0.5$. The simulation times for each value of λ varied from 250 ps to 1250 ps depending on the degree of convergence obtained. In Fig. 1 the behaviour of the free energy derivative as a function of λ is illustrated for propane in 6.9 M urea together with the respective errors obtained from block averaging.[50]

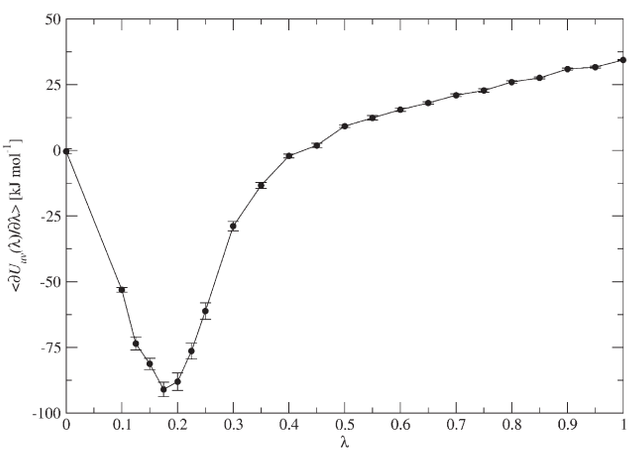

Fig. 1 Free energy derivative of solvating propane in 6.9 M urea–water. The error bars were obtained from block averaging. Simulation times per λ-point ranged between 250 ps to 1250 ps.

In addition to the free enthalpy of solvation ΔG_S we have calculated the solute–solvent energy ΔU_{uv}, which reflects the energy change due to establishing interactions between the solute and the surrounding solvent molecules, and the solute–solvent entropy ΔS_{uv}, which expresses a reduction of the configurational freedom of the solvent by having a solute present at some fixed position. This is an excluded volume effect in case of non-polar solutes. The solute–solvent energy and entropy TI formulae are:[40,51]

$$\Delta U_{uv} = \langle U_{uv}(\lambda = 1)\rangle_{\lambda=1} \tag{3}$$

and

$$T\Delta S_{uv} = \frac{1}{kT}\int_0^1 \mathrm{d}\lambda \left[\langle U_{uv}(\lambda)\rangle_\lambda \left\langle \frac{\partial}{\partial\lambda} U_{uv}(\lambda)\right\rangle_\lambda - \left\langle U_{uv}(\lambda)\frac{\partial}{\partial\lambda} U_{uv}(\lambda)\right\rangle_\lambda\right]. \tag{4}$$

In eqn. (4), k denotes Boltzmann's constant and T is the temperature. The solvation enthalpy and entropy contain-in addition to the solute–solvent contributions (3) and (4)-a solvent reorganization term that quantifies the change of the solvent–solvent energy due to the formation of a molecular-sized cavity in the solvent. However, this contribution adds to the solvation enthalpy and entropy in such a way that it exactly compensates in the solvation free energy,[40,51] which therefore reads

$$\Delta G_S = \Delta U_{uv} - T\Delta S_{uv}. \tag{5}$$

Although the change of the solvent potential energy due to solute insertion has no direct effect on ΔG_S, the nature of solvent–solvent interactions in the liquid are of prime importance in rationalising ΔG_S. Because the solvent potential energy enters eqns. (3) and (4) through the NPT ensemble averages, it affects ΔU_{uv} and $T\Delta S_{uv}$ only indirectly. Solvent–solvent interactions determine the solvent density. In denser solvents, ΔU_{uv} and ΔS_{uv} may take larger negative values. Moreover, the solvent–solvent interactions determine the capacity or "flexibility" of the solvent to open up molecular-sized cavities of the proper size and shape to accommodate the solute. This molecular-scale flexibility has shown to be a determinant factor affecting the probability of finding a suitable cavity[52,53] and may determine the magnitude and sign of the solute–solvent entropy change in solute transfer processes between liquid solvent phases.[39]

3. Results and discussion

Thermodynamic analysis

The thermodynamic solvation quantities of the aliphatic solutes and the respective effective hydrocarbon solute diameter[30] are shown in Table 1 The first block contains the simulated (computed through eqn. (2)) and experimental (obtained by combining the values of transfer to neat water[30] and from water to aqueous urea[31]) solvation free energies in 6.9 M urea–water mixture. In the second block are displayed the simulated[39,43] and experimental[30] solvation free energies for neat water. The third block shows the measured[36] and calculated transfer free energies of the aliphatic hydrocarbons from water to 6.9 M aqueous urea. In addition, solute–solvent energy (computed using eqn. (3)) and entropy components (computed using eqns. (2) and (5)) are included. Calculating the entropy components through eqn. (4) yields only small differences compared to using eqns. (2) and (5). The entropy values differ on average by 0.5 kJ mol^{-1}, with the largest difference being 1.5 kJ mol^{-1} for *i*-butane.

The simulated ΔG_S values in 6.9 M urea are slightly too low (the solubilities are overestimated). The discrepancy between the calculated results and the experimental values amounts to 0.3 kJ mol^{-1} for methane and about 1–2 kJ mol^{-1} for the larger hydrocarbons. The statistical error in the TI calculations is approximately 1 kJ mol^{-1}, whereas for methane, whose solvation quantities were calculated with TPI, the error is one order of magnitude smaller. The dependence of the solvation free energies on the solute size is presented in Fig. 2. The experimental trends in both water and 6.9 M urea are well reproduced and have a so-called V-shape characteristic for hydrocarbon solvation in water and aqueous urea.[31] The bottom panel in Fig. 2 shows the hydrocarbon transfer free energies. Since in pure water the hydration free energies are well reproduced and the salting-in effects caused by addition of urea are overestimated, the calculated transfer free energies $\Delta\Delta G_S = \Delta G_S(6.9\ \mathrm{M\ urea}) - \Delta G_S(\mathrm{pure\ water})$ are too low. The simulated values (full line) are shifted down by about 1–2 kJ mol^{-1} in comparison with the experimental transfer data (dashed line). As a result, our model predicts salting-in for hydrocarbons larger than methane instead for those larger than ethane which is observed experimentally.

The solute–solvent energy $\Delta\Delta U_{uv}$ and entropy changes $T\Delta\Delta S_{uv}$ of solute transfer are also shown in Table 1 For all solutes, the transfer process is favoured by the solute–solvent energy change while being opposed by the change of solute–solvent entropy. We again note that the experimental solvation entropies and enthalpies[31] are both positive indicating an apparent entropy-driven salting-in by urea. The solvation enthalpy and entropy, however, contain, in addition to the solute–solvent contributions calculated here, exactly compensating solvent–solvent (solvent reorganisation) terms. It is not possible to calculate the value of these terms to a reasonable degree of accuracy, since they are ensemble averages over all solvent degrees of freedom.[54] The entropic opposition to solvation, $T\Delta\Delta S_{uv}$, will be negative, if by addition of urea to water the flexibility of the medium with regard to spontaneous opening up of suitable solute cavities decreases.[40] This quantity would have had a positive sign, on the other hand, if

Table 1 Thermodynamic quantities in kJ mol^{-1} (at 298 K and 1 atm) associated with the solvation of aliphatic hydrocarbons. σ denotes the hard-sphere diameter[30] in nm. ΔU_{uv}: solute–solvent potential energy (eqn. (3)). ΔS_{uv}: solute–solvent entropy (eqns. (2) and (5)). ΔG_S: free enthalpy of solvation (eqn. (2))

		6.9 M urea–water				Water				Transfer			
		ΔU_{uv}	$T\Delta S_{uv}$	ΔG_S		ΔU_{uv}	$T\Delta S_{uv}$	ΔG_S		$\Delta\Delta U_{uv}$	$T\Delta\Delta S_{uv}$	$\Delta\Delta G_S$	
Solute	σ	sim	sim	exp	sim	sim	sim	exp[30]	sim[43]	sim	sim	exp[36]	sim
Methane	0.370	−15.8	−24.6	9.1	8.8	−13.5	−22.2	8.3	8.7[39]	−2.3	−2.4	0.8	0.1
Ethane	0.438	−25.9	−32.6	8.0	6.7	−21.7	−29.1	7.6	7.4	−4.2	−3.5	0.4	−0.7
Propane	0.506	−34.4	−40.8	8.1	6.4	−29.3	−37.9	8.2	8.6	−5.1	−2.9	−0.1	−2.2
i-Butane	0.555	−39.3	−47.4	9.2	8.1	−35.0	−45.3	9.7	10.3	−4.3	−2.1	−0.5	−2.2
n-Butane	0.565	−44.0	−50.1	8.2	6.1	−36.4	−45.1	8.7	8.7	−8.6	−6.0	−0.5	−2.6
Neo-pentane	0.589	−48.3	−55.8	9.8	7.5	−39.9	−49.8	10.5	9.9	−8.4	−6.0	−0.7	−2.4

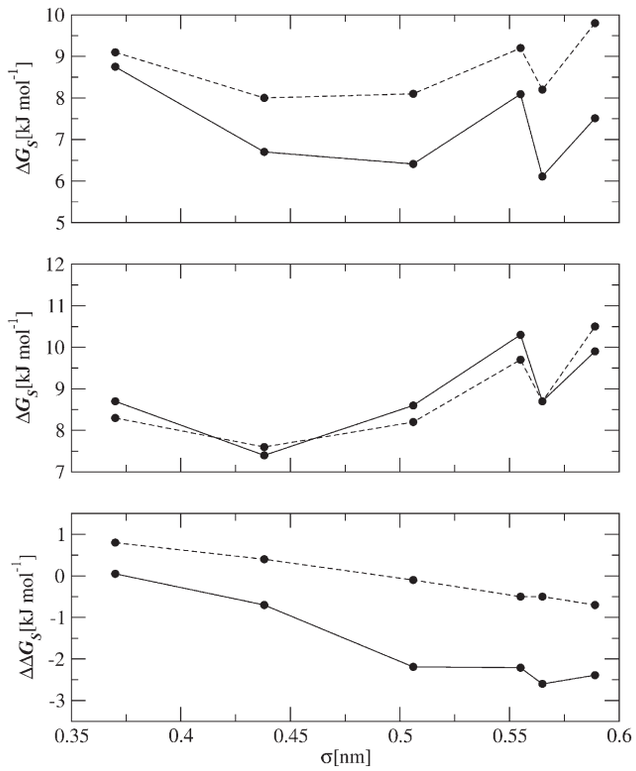

Fig. 2 Solvation free energies of aliphatic hydrocarbons in 6.9 M urea–water mixture (upper panel), in neat water (middle panel) presented *versus* the hydrocarbon diameter σ. The transfer free energies from water to 6.9 M urea–water are shown in the lower panel. Simulation: solid lines. Experiment: dashed lines. See also Table 1.

due to weak urea–water interactions the medium could create empty molecular-sized cavities more easily. This molecular scale flexibility largely depends on the strength of the interactions between solvent components. When, for example, sodium chloride is added to water, strong ion–water interactions hamper spontaneous opening of cavities close to hydrated ions, which leads to an entropy-driven salting-out of non-polar solutes.[39] Cavities in sodium chloride/water are preferentially hydrated,[39] because bulk water very efficiently reorganises close to small cavities, whereas ion hydration waters cannot. In aqueous urea the solute–solvent entropy change favours the salting-out of non-polar solutes too, were it not for the fact that this effect is overcompensated by a favourable solute–solvent energy of urea interaction with the solute leading to the observed salting-in effect. In analogy to what happens in sodium chloride/water one may postulate that urea is strongly hydrated, inhibiting the formation of solute-sized cavities close to urea molecules. Yet, solute–urea interactions are energetically favourable causing solute association with urea being entropically more expensive compared to a situation in which the solute is preferentially hydrated, *i.e.* direct solute–urea interactions compete with strong water–urea hydrogen bonding interactions. Therefore, solute–urea association occurs at the expense of a strong excluded volume (entropy) penalty. In the next section we confirm the picture established here by analysing the solvent structure close to the hydrocarbons and to repulsive hydrocarbon cavities. Our simulation results yield a microscopic picture that supports the conclusions previously drawn by other authors[24,31,36] that the addition of urea enhances the hydrophobic effect for small solutes (entropy dominates) but weakens it for the larger ones (energy dominates).

Structural analysis

Fig. 3 depicts the solute–solvent radial distribution functions $g(r)$ for water (dashed lines) and urea (solid lines) molecules

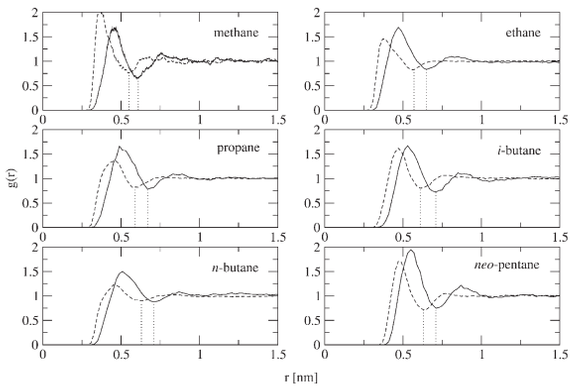

Fig. 3 Hydrocarbon/solvent radial distribution functions $g(r)$ (urea: solid lines, water: dashed lines). The atoms involved are the most central atoms of the hydrocarbons, the urea carbon and the water oxygen. The vertical dotted lines indicate the integration limit used in evaluating first shell coordination numbers, for urea (n_u) and water (n_w) given in Table 2.

around the aliphatic hydrocarbons. The atoms chosen for computing the $g(r)$'s were the water oxygen, the urea carbon and the most central hydrocarbon atom. All hydrocarbons show a very well defined first-shell solvation peak for each of the two mixture components with the urea peak being higher for ethane, propane, *n*-butane, and neo-pentane. The water peaks are narrow and sharp for methane, *i*-butane and neo-pentane. This shows that water packs around those solutes in a well defined shell. However, for the less spherical aliphatic solutes (ethane, propane, and *n*-butane) the water distribution is less narrow. This broadening, although less distinct, is also observed for the urea peaks that are generally higher and wider than the water peaks for the hydrocarbons larger than methane. To obtain a better picture of what is happening at the molecular level we have integrated the distribution functions up to the first solvation shell inclusive whose radius is depicted by the dotted vertical lines in Fig. 3. The first shell coordination numbers and their ratios are listed in the first three columns of Table 2 The urea/water ratio increases slightly with increasing solute size. Except for methane and *i*-butane, the values are slightly larger compared to the situation in which n_u/n_w is calculated using a random point in the liquid, rather than the solute itself, to define the origin (fourth column). Therefore, a weakly preferential direct urea–solute interaction occurs in these systems. To further examine preferential solute–urea binding, we have calculated excess coordination numbers from the evaluation of KB integrals (eqn. (1)). These results are presented in the fifth and sixth column of Table 2 for urea and water, respectively. Preferential binding parameters $\nu = \rho_u(G_{Su} - G_{Sw})$ are listed in the last column and are positive except for methane and *i*-

Table 2 Hydrocarbon solute first shell coordination numbers n_u for urea and n_w for water, Kirkwood–Buff excess coordination numbers $\rho_u G_{su}$ and $\rho_w G_{sw}$ and preferential binding parameter $\nu = \rho_u(G_{su} - G_{sw})$. The ratios n_u/n_w are given for first shell coordination numbers around a hydrocarbon "solute" and around a "random" point in the solution

Solute	n_u solute	n_w solute	n_u/n_w solute	n_u/n_w random	$\rho_u G_{Su}$ solute	$\rho_w G_{Sw}$ solute	ν solute
Methane	3.3	15.2	0.22	0.25	−0.17	−0.77	−0.03
Ethane	4.8	16.6	0.29	0.26	−0.13	−2.28	0.28
Propane	5.3	18.3	0.29	0.27	0.01	−2.77	0.51
i-butane	5.8	20.5	0.28	0.28	−0.87	−1.08	−0.67
n-butane	6.6	20.7	0.32	0.26	2.80	−10.99	4.78
Neo-pentane	6.3	21.0	0.30	0.26	0.33	−5.18	1.27

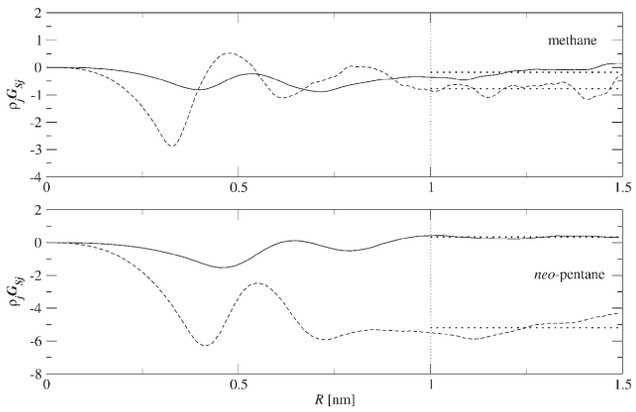

Fig. 4 Excess coordination number $\rho_j G_{Sj}$ of urea (j = u, solid lines) and water (j = w, dashed lines) as a function of the distance R to methane (top panel) and neo-pentane (bottom panel). The values for $\rho_j G_{Sj}$ shown in Table 2 have been obtained using the average (thick dotted line) over the range 1.0–1.5 nm.

butane. Because the KB integrals converge slowly with increasing integration distance R, we have used the average value of G_{Sj} between 1.0–1.5 nm in order to average out long-range noise. As an example, Fig. 4 shows excess urea (solid lines) and water (dashed lines) coordination numbers as a function of the integration distance R_c (eqn. (1)) for methane and neo-pentane. The horizontal lines indicate the average coordination numbers in the range from 1.0 to 1.5 nm. Preferential urea interaction with neo-pentane occurs through direct (small R) as well as indirect (large R) contributions while water is expelled at all distances R. For the other solutes, urea excess coordination numbers oscillate around zero with increasing R, and converge to a positive value at distances larger than 1.0 nm. For water the excess coordination numbers are all negative and lower than the values for urea. These results lead us to conclude that water is expelled by the solute whereas urea tends to weakly bind the hydrocarbon.

Because the direct solute–urea interaction results from a favourable van der Waals energy change ($\Delta\Delta U_{uv} < 0$), it is of interest to investigate how repulsive hydrocarbon cavities are solvated. The cavities can be obtained by switching off the attractive C_6-term in the van der Waals interactions in the simulations. Solvation of solutes with only the excluded volume (C_{12}-) part of the hydrocarbon-solvent interaction involves breaking of solvent–solvent interactions without providing in return an attractive solute–solvent interaction. The solvation structure of repulsive hydrocarbon cavities provides information on local solvent environments for which cavity formation is most likely to occur. The cavity-solvent radial distribution functions obtained are shown in Fig. 5. All cavities are preferentially hydrated. In other words, cavities are created more easily in the vicinity of water molecules rather than urea indicating that urea is strongly hydrated in comparison to the hydration of a water molecule in bulk water. The cavity-solvent $g(r)$'s show a strong urea expulsion from the first as well as from the second solvation shell. Table 3 shows the first shell cavity coordination numbers n_u and n_w. The ratio n_u/n_w ("cavity") has decreased significantly over the situation in which the attractive part of the van der Waals interaction was present ("solute") (Table 2). We note that the values of n_u/n_w at random positions are different between Table 2 and Table 3, because the radii of the first solvation shell of the solutes (Fig. 3) differ from those of the cavities (Fig. 5). The excess water coordination numbers obtained from the KB analysis have increased indicating that cavities are preferentially hydrated. Hence, based on solute excluded volume arguments only, aliphatic hydrocarbons are preferentially hydrated in 6.9 M urea. The attractive van der Waals solute–solvent energy, however, drives association of urea with the hydrocarbon solutes. The latter process occurs at the expense of a negative entropy change ($T\Delta\Delta S_{uv} < 0$).

4. Conclusions

We have calculated solvation thermodynamic quantities of six aliphatic hydrocarbons in 6.9 M aqueous urea using molecular dynamics simulation. Solvation free energies were obtained and analysed for non-polar molecules of increasing size: methane, ethane, propane, *i*-butane, *n*-butane and neo-pentane. The transfer free energies of the hydrocarbons from water to the mixture were also computed. Our results compare

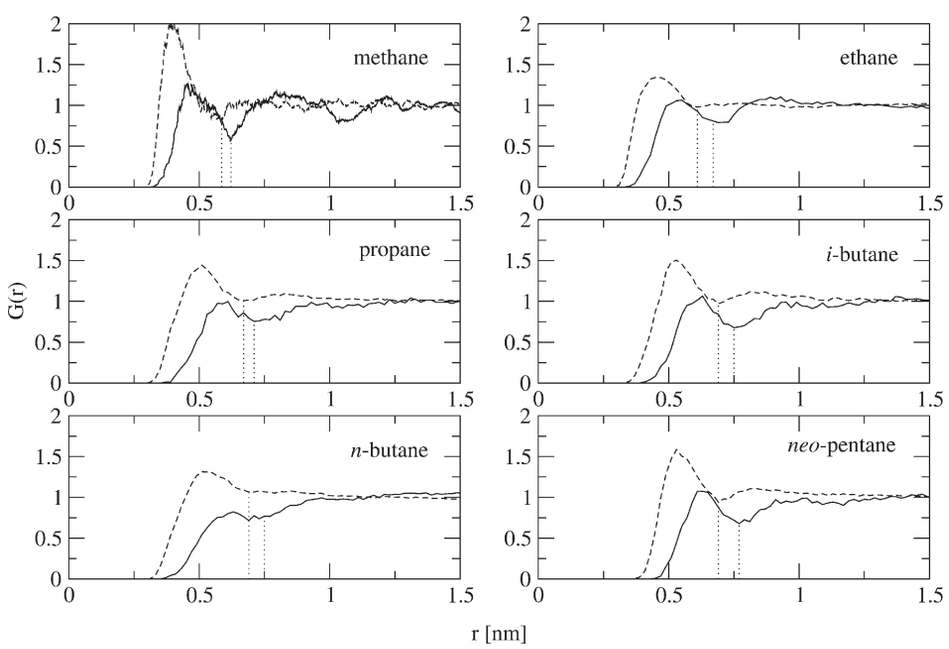

Fig. 5 Hydrocarbon-cavity/solvent radial distribution functions $g(r)$ (urea: solid lines, water: dashed lines). The atoms involved are the most central atoms of the hydrocarbons, the urea carbon and the water oxygen. The vertical dotted lines indicate the integration limit used in evaluating first shell coordination numbers, for urea (n_u) and water (n_w) given in Table 3.

Table 3 Hydrocarbon solute cavity first shell coordination numbers n_u for urea and n_w for water, Kirkwood–Buff excess coordination numbers $\rho_u G_{su}$ and $\rho_w G_{sw}$ and preferential binding parameter $\nu = \rho_u(G_{su} - G_{sw})$. See also caption of Table 2

Cavity	n_u cavity	n_w cavity	n_u/n_w cavity	n_u/n_w random	$\rho_u G_{Su}$ cavity	$\rho_w G_{Sw}$ cavity	ν cavity
Methane	2.9	18.7	0.16	0.20	−1.69	−1.50	−1.96
Ethane	3.8	21.4	0.18	0.24	−1.36	−1.36	−1.11
Propane	3.9	28.7	0.14	0.22	−4.10	4.58	−4.92
i-Butane	4.5	30.4	0.15	0.23	−4.70	4.74	−5.56
n-Butane	4.2	31.1	0.14	0.23	−3.88	2.45	−4.32
Neo-pentane	4.8	29.7	0.16	0.25	−5.04	4.52	−5.86

well with the experimental data, the discrepancies being within kT. The calculations also reproduce the V-shape observed in the free energy as a function of increasing hydrocarbon size. A decomposition of the free energy into the pertinent entropic and energetic contributions has shown that the solute–solvent entropy opposes the transfer process whereas the solute–solvent energy favours it. For small solutes (methane) the solute–solvent entropy change dominates and the transfer is unfavourable. With increasing solute size, the attractive van der Waals solute–solvent energy compensates for an unfavourable solute–solvent entropy change, which causes the free energy to change sign and the transfer process to become favourable. Our results support the previous work by Graziano,[31] who achieved the same conclusions by a different approach. A structural analysis of the molecular dynamics trajectories provided additional information about the interaction between urea and the solutes. Solute–solvent radial distribution functions were analysed to see how the composition of the solvation shells of the solutes changes with solute size and shape. Less spherical solute shapes yield broader and less well defined peaks, whereas the more symmetrical solute shapes yield narrow and sharp peaks. The excess coordination numbers of solvent components obtained by computing the Kirkwood–Buff integrals show a weak preferential binding of urea to the non-polar solutes. In addition, the solvation structure of repulsive hydrocarbon cavities was analysed by switching off the attractive van der Waals term in the hydrocarbon-solvent interaction. In this case hydrocarbon-sized cavities occur more often in the vicinity of water rather than of urea molecules. Based on this evidence and the fact that with the full interaction a direct urea association with the solute is observed, we conclude that solute co-solvent binding is promoted by an attractive van der Waals interaction while being entropically opposed due to strong urea hydration.

Acknowledgements

This work is financially supported by the Swiss National Centre of Competence in Research (NCCR) in Structural Biology and the Swiss National Science Foundation (SNF).

References

1 P. P. Kamoun, *Trends Biochem. Sci.*, 1988, **13**, 424.
2 A. Wallqvist, D. G. Covell and D. Thirumalai, *J. Am. Chem. Soc.*, 1998, **120**, 427.
3 D. Tobi, R. Elber and D. Thirumalai, *Biopolymers*, 2003, **68**, 359.
4 R. D. Mountain and D. Thirumalai, *J. Am. Chem. Soc.*, 2003, **125**, 1950.
5 Q. Zou, S. M. Habermann-Rottinghaus and K. P. Murphy, *Proteins*, 1998, **31**, 107.
6 B. J. Bennion and V. Daggett, *Proc. Natl. Acad. Sci. USA*, 2003, **100**, 5142.
7 E. S. Boek, W. J. Briels, J. van Eerden and D. Feil, *J. Chem. Phys.*, 1992, **96**, 7010.
8 E. S. Boek and W. J. Briels, *J. Chem. Phys.*, 1993, **98**, 1422.
9 J. Hernandez-Cobos, I. Ortega-Blake, M. Bonilla-Marin and M. Moreno-Bello, *J. Chem. Phys.*, 1993, **99**, 9122.
10 P. O. Astrand, A. Wallqvist and G. Karlstrom, *J. Chem. Phys.*, 1994, **100**, 1262.
11 P. O. Astrand, A. Wallqvist and G. Karlstrom, *J. Phys. Chem.*, 1994, **98**, 8224.
12 J. Tsai, M. Gerstein and M. Levitt, *J. Chem. Phys.*, 1996, **104**, 9417.
13 M. Levitt, M. Hirshberg, R. Sharon and V. Daggett, *Comput. Phys. Commun.*, 1995, **91**, 215.
14 R. Chitra and P. E. Smith, *J. Phys. Chem. B*, 2000, **104**, 5854.
15 J. J. V. Cirino and C. A. Bertran, *Quim. Nova*, 2002, **25**, 358.
16 C. A. Bertran, J. J. V. Cirino and L. C. G. Freitas, *J. Braz. Chem. Soc.*, 2002, **13**, 238.
17 L. G. Dias, F. H. Florenzano, W. F. Reed, M. S. Baptista, S. M. B. Souza, E. B. Alvarez, H. Chaimovich, I. M. Cuccovia, C. L. C. Amaral, C. R. Brasil, L. S. Romsted and M. J. Politi, *Langmuir*, 2002, **18**, 319.
18 F. Sokolic, A. Idrissi and A. Perera, *J. Chem. Phys.*, 2002, **116**, 1636.
19 E. M. Duffy, D. L. Severance and W. L. Jorgensen, *Isr. J. Chem.*, 1993, **33**, 323.
20 L. J. Smith, H. J. C. Berendsen and W. F. van Gunsteren,*J. Phys. Chem. A*, 2004, in press.
21 J. Tirado-Rives, M. Orozco and W. L. Jorgensen, *Biochemistry*, 1997, **36**, 7313.
22 A. Caflisch and M. Karplus, *Struct. Fold. Des.*, 1999, **7**, 477.
23 Z. Y. Zhang, Y. J. Zhu and Y. Y. Shi, *Biophys. Chem.*, 2001, **89**, 145.
24 M. Ikeguchi, S. Nakamura and K. Shimizu, *J. Am. Chem. Soc.*, 2001, **123**, 677.
25 E. M. Duffy, P. J. Kowalczyk and W. L. Jorgensen, *J. Am. Chem. Soc.*, 1993, **115**, 9271.
26 N. T. Southall, K. A. Dill and A. D. J. Haymet, *J. Phys. Chem. B*, 2002, **106**, 521.
27 H. S. Frank and M. W. Evans, *J. Chem. Phys.*, 1945, **13**, 507.
28 B. Lee, *Biopolymers*, 1985, **24**, 813.
29 B. Lee, *Biopolymers*, 1991, **31**, 993.
30 G. Graziano, *J. Chem. Soc.-Faraday Trans.*, 1998, **94**, 3345.
31 G. Graziano, *J. Phys. Chem. B*, 2001, **105**, 2632.
32 G. Graziano, *Can. J. Chem.*, 2002, **80**, 388.
33 G. Graziano, *Can. J. Chem.*, 2002, **80**, 401.
34 B. Lee, *Biophys. Chem.*, 1994, **51**, 271.
35 L. Liu and Q. X. Guo, *Chem. Rev.*, 2001, **101**, 673.
36 D. B. Wetlaufer, R. L. Coffin, S. K. Malik and L. Stoller, *J. Am. Chem. Soc.*, 1964, **86**, 508.
37 J. G. Kirkwood and F. P. Buff, *J. Chem. Phys.*, 1951, **19**, 774.
38 A. Ben-Naim, *Solvation Thermodynamics*, Plenum Press, New York, 1987.
39 N. F. A. van der Vegt and W. F. van Gunsteren, *J. Phys. Chem. B*, 2004, in press.
40 N. F. A. van der Vegt, D. Trzesniak, B. Kasumaj and W. F. van Gunsteren, *ChemPhysChem*, 2004, in press.
41 W. F. van Gunsteren, S. R. Billeter, A. A. Eising, P. H. Hünenberger, P. Krüger, A. E. Mark, W. R. P. Scott and I. G. Tironi, in *Biomolecular Simulation: The GROMOS96 Manual and User Guide*, Zürich, 1996.
42 H. J. C. Berendsen, J. P. M. Postma, W. F. van Gunsteren and J. Hermans, *Intermolecular Forces*, ed. B. Pullman, Reidel, 1981.
43 L. D. Schuler, X. Daura and W. F. van Gunsteren, *J. Comput. Chem.*, 2001, **22**, 1205.
44 J. P. Ryckaert, G. Ciccotti and H. J. C. Berendsen, *J. Comput. Phys.*, 1977, **23**, 327.
45 H. J. C. Berendsen, J. P. M. Postma, W. F. van Gunsteren, A. Dinola and J. R. Haak, *J. Chem. Phys.*, 1984, **81**, 3684.
46 P. E. Smith and W. F. van Gunsteren, *J. Chem. Phys.*, 1994, **100**, 3169.
47 J. G. Kirkwood, *J. Chem. Phys.*, 1935, **3**, 300.
48 W. F. van Gunsteren, X. Daura and A. E. Mark, *Helv. Chim. Acta*, 2002, **85**, 3113.
49 T. C. Beutler, A. E. Mark, R. C. van Schaik, P. R. Gerber and W. F. van Gunsteren, *Chem. Phys. Lett.*, 1994, **222**, 529.
50 X. Daura, P. H. Hünenberger, A. E. Mark, E. Querol, F. X. Aviles and W. F. van Gunsteren, *J. Am. Chem. Soc.*, 1996, **118**, 6285.
51 H. A. Yu and M. Karplus, *J. Chem. Phys.*, 1988, **89**, 2366.
52 L. R. Pratt, *Annu. Rev. Phys. Chem.*, 2002, **53**, 409.
53 A. Pohorille and L. R. Pratt, *J. Am. Chem. Soc.*, 1990, **112**, 5066.
54 C. Peter, B. C. Oostenbrink, A. van Dorp and W. F. van Gunsteren, *J. Chem. Phys.*, 2003, in press.

